Mixed-Valence and Neutral Framework Inorganic−Organic Hybrid Materials: Synthesis, Characterization, and Magnetic Properties of $[\{Co(N(CH)_4N)\}(V_2O_5)_2]$ and $[\{Co(N(CH)_4N)\}V_2O_6]$

M. Ishaque Khan,*[,†] Elizabeth Yohannes,[†] Vladimir O. Golub,[‡] Charles J. O'Connor,[‡] and Robert J. Doedens*[,§]

Department of Biological, Chemical, and Physical Sciences, Illinois Institute of Technology, Chicago, Illinois 60616, Department of Chemistry, University of New Orleans, New Orleans, Louisiana 70148, and Department of Chemistry, University of California, Irvine, California 92697

Received May 24, 2007. Revised Manuscript Received July 30, 2007

Two inorganic−organic hybrid materials $[\{Co(N(CH)_4N)\}(V_2O_5)_2]$ (**1**) and $[\{Co(N(CH)_4N)\}V_2O_6]$ (**2**) have been synthesized and characterized by FT-IR spectroscopy, thermogravimetric analysis, elemental analysis, manganometric titration, temperature-dependent magnetic susceptibility measurement, bond valence sum calculations, and single-crystal X-ray diffraction analyses. The neutral framework materials were prepared by the amalgamation of vanadium oxide chains and layers with metal−organoamine coordination polymers. The three-dimensional framework structures of the crystals in **1** and **2** are composed of vanadium oxide layers (**1**) and chains (**2**) combined with $\{Co(N(CH)_4N)\}^{2+}$ motifs that cross-link the reduced vanadium oxide layers (containing mixed-valent vanadium centers) in **1** and oxovanadium chains in **2**. Besides crosslinking the metal oxide chains and layers in these materials, cationic metal−pyrazine polymers provide charge balance leading to the neutral framework in these solids. The compounds show good thermal stability. Crystal data for **1** is as follows: $C_4H_4N_2O_{10}CoV_4$, orthorhombic space group *Cmcm*, $a = 14.3071(6)$, $b = 6.9965(3)$, $c = 11.4510(5)$ Å, $V = 1146.24(9)$ Å^3, $Z = 4$, $D_{calcd} = 2.913$ Mg·m^{-3}, R1 = 0.0385 (all data), wR2 = 0.1019. Crystal data for **2** are as follows: $C_4H_4N_2O_6CoV_2$, orthorhombic space group *Pnna*, $a = 10.2524(8)$, $b = 11.5653(9)$, $c = 7.4719(6)$ Å, $V = 885.96(12)$ Å^3, $Z = 4$, $D_{calcd} = 2.526$ Mg·m^{-3}, R1 = 0.0199 (all data), wR2 = 0.0547.

Introduction

Inorganic−organic hybrid materials are of fundamental and practical interest.[1,2] Such materials can exhibit properties (structural, electronic, catalytic, sorbtive, gas storage, etc.) that are not commonly observed in purely inorganic or organic phases. Furthermore, the properties and performance of hybrid materials can potentially be improved and/or fine-tuned by incorporating suitable functionalities.[3−8]

Several synthetic approaches have been adopted for preparing hybrid materials in recent years. The "modular chemistry" approach,[9] which exploits secondary building units as the basis for assembling extended structure solids, has led to the synthesis of a prominent class of metal−organic framework materials.[3,10−12] Another useful synthetic approach involves the combination of metal oxides with organic ligands along with other heterometal centers. This approach has yielded an impressive class of organic−transition metal oxide hybrids constructed from molybdenum oxide motifs and metal−organic complexes.[13−16]

We have been interested in the design and synthesis of hybrid framework materials by amalgamation of vanadium oxide based structures with metal−organic compounds and

* Corresponding authors. E-mail: khan@iit.edu.
† Illinois Institute of Technology.
‡ University of New Orleans.
§ University of California.

(1) *Hybrid Materials: Synthesis, Characterization, and Applications*; Kickelbick, G., Ed.; Wiley-VCH: Weinheim, 2007.
(2) (a) Horcajaba, P.; Serre, C.; Regi, M. V.; Sebban, M.; Taulelle, F.; Ferez, G. *Angew. Chem., Int. Ed.* **2006**, *45*, 5974−5978. (b) Hupp, J. T.; Poeppelmeier, K. R. *Science* **2005**, *309*, 2008−2009.
(3) Eddaoudi, M.; Moler, D.; Li, H.; Chen, B.; Reineke, T.; O'Keeffe, M.; Yaghi, O. *Acc. Chem. Res.* **2001**, *34*, 319−330 and references therein.
(4) Kitagawa, S.; Kitaura, R. *Comments Inorg. Chem.* **2002**, *23*, 101−126.
(5) Lee, E. Y.; Jang, S. Y.; Suh, M. P. *J. Am. Chem. Soc.* **2005**, *127*, 6374−6381.
(6) Seo, J. S.; Whang, D.-M.; Lee, H.-Y.; Jun, S. I.; Oh, J.-H.; Jeon, Y.-J.; Kim, K. *Nature* **2000**, *404*, 982−986.
(7) Wu, C.-D.; Hu, A.; Zang, L.; Lin, W. *J. Am. Chem. Soc.* **2005**, *127*, 8940−8941.
(8) Albrecht, M.; Lutz, M.; Spek, A. L.; Van Koten, G. *Nature* **2000**, *406*, 970−974.
(9) *Modular Chemistry*; Michl, J., Ed.; Kluwer Academic Publishers: Dordrecht, 1995 (and references therein).
(10) Yaghi, O. M.; Li, H.; Davis, C.; Richardson, D.; Groy, T. L. *Acc. Chem. Res.* **1998**, *31*, 474−484 and references therein.
(11) Eddaoudi, M.; Li, H.; M.; Yaghi, O. *J. Am. Chem. Soc.* **2000**, *122*, 1391−1397.
(12) Chen, B.; Eddaoudi, M.; Hyde, S.; O', Keeffe, M.; Yaghi, O. *Science* **2001**, *291*, 1021−1023.
(13) Hagrman, D.; Warren, C. J.; Haushalter, R. C.; Seip, C.; O' Connor, C. J.; Rarig, J. R. L.; Johnson, K. M.; Laduca, J. R. L.; Zubieta, J. *Chem. Mater.* **1998**, *10*, 3294−3297.
(14) Hagrman, P. J.; Hagrman, D.; Zubieta, J. *Angew. Chem., Int. Ed.* **1999**, *38*, 2638−2684 and references therein.
(15) Zapf, P. J.; Warren, C. J.; Haushalter, R. C.; Zubieta, J. *Chem. Commun.* **1997**, 1543.
(16) (a) Hagrman, D.; Haushalter, R. C.; Zubieta, J. *Chem. Mater.* **1998**, *10*, 361. (b) Hagrman, D.; Zubieta, J. *J. Solid State Chem.* **2000**, *152*, 141. (c) Hagrman, D.; Zubieta, C.; Rose, D. J.; Zubieta, J. *Angew. Chem., Int. Ed.* **1997**, *36*, 873. (d) Hagrman, D.; Zubieta, J. *Chem. Commun.* **1998**, 2005−2006. (e) Zapf, P. J.; Hammond, R. P.; Haushalter, R. C.; Zubieta, J. *Chem. Mater.* **1998**, *10*, 1366−1373.

10.1021/cm071415n CCC: $37.00
Published on Web 09/08/2007

their coordination polymers.[17−24] Besides forming a rich class of polyoxovanadate clusters, vanadium also forms a variety of oxovanadate chains and layered structures composed of $\{VO_4\}$ tetrahedra and $\{VO_5\}$ square pyramids, respectively.[25−27] They provide attractive building block units for the construction of new structures and framework materials. Unlike the aluminosilicate frameworks commonly observed in conventional zeolites[28−29] that are derived from tetrahedral $\{SiO_4\}$ and $\{AlO_4\}$ building block units of the main group elements, vanadium oxide based framework materials can exhibit a variety of metal oxidation states, variable coordination numbers, and diverse geometries around the vanadium. These features could provide a basis for new types of catalytic and sorbtive behavior in such materials.

We have developed synthetic strategies that employ vanadium oxide chains and layers as pre-organized building units and simple metal−organic complexes as cross-linkers. We have been focusing on synthesis of mixed metal oxide hybrid framework materials where metal−organoamine cationic complexes serve as cross-linkers of the vanadium oxide chains and layers besides providing the charge balance needed for generating a neutral framework.

During the course of this research effort,[17−24] we have discovered new porous framework materials of unprecedented structures composed of vanadium oxide and metal−organoamine coordination polymers. Here we describe the synthesis of two novel open framework hybrid materials, $[\{Co(N(CH)_4N)\}(V_2O_5)_2]$ (**1**) and $[\{Co(N(CH_2)_4N)\}V_2O_6]$ (**2**), and their characterization by infrared spectroscopy, thermogravimetry, elemental analysis, manganometric titration, bond valence sum calculations, temperature-dependent magnetic susceptibility measurement, and single-crystal X-ray structure analyses.

Experimental Section

Materials and Methods. All chemicals used in this work were purchased from commercial sources and used without further purification. Infrared spectra (KBr pellet; 4000−400 cm^{-1} region) were recorded on a Perkin-Elmer Paragon 1000 FT-IR spectrometer. Thermogravimetric analysis (TGA) was performed on a Universal V2.5H thermal analyzer. Typically, 20−30 mg of sample was placed in a quartz bucket and heated in argon flow of 50 mL/min with a heating rate of 5°/min. The residues from the TGA experiments were examined by IR spectroscopy. Redox titrations were performed on a Mettler Toledo DL12 titrator using dilute acidic solutions of the compounds against standardized $KMnO_4$ solution. Elemental analyses were performed on Perkin-Elmer 2400 elemental analyzer, and a Perkin-Elmer Optima 3300DC DCP spectrometer.

The magnetic susceptibility data were recorded on a 25.16 mg crystalline sample of $[\{Co(N(CH)_4N)\}(V_2O_5)_2]$ (**1**) in the 2−300 K temperature range using a Quantum Design MPMS-5S SQUID spectrometer. The calibrating and operating procedures were done according to the literature method.[30] Temperature-dependent magnetic data were obtained at a magnetic field $H = 1000$ Oe.

Synthesis of $[\{Co(N(CH)_4N)\}(V_2O_5)_2]$ (1). A mixture of V_2O_5 (1.25 mmol), $LiOH{\cdot}H_2O$ (2.5 mmol), pyrazine (1.87 mmol), $CoSO_4{\cdot}7H_2O$ (1.87 mmol), and H_2O (555.55 mmol) in the molar ratio of 1:2:1.5:1.5:444 was placed in a 23 mL Teflon-lined Parr autoclave. The mixture was stirred for 30 s and heated for 96 h at 180 °C inside an electric furnace. After the autoclave was cooled to room temperature for 3 h, black rod-like and black rectangular block shaped crystals mixed with a reddish brown microcrystalline impurity were filtered from lighter brown mother liquor. Crystals were washed thoroughly with methanol and then with deionized water and dried in air at room temperature. The black rod-like and rectangular block-shaped crystals, which gave identical infrared spectra and other analytical data, were separated mechanically from the reddish brown microcrystalline phase to give 60.5 mg of $[\{Co(N(CH)_4N)\}(V_2O_5)_2]$ (**1**; ∼29% based on vanadium). Anal. Calcd for $C_4H_4N_2O_{10}CoV_4$ (**1**): C, 9.56; H, 0.8; N 5.57; Co, 11.72; V, 41.29. Found: C, 9.63; H, 0.90; N 5.55; Co, 11.19; V, 40.53. Prominent IR bands (KBr pellet, 4000−400 cm^{-1}): 1417 (m), 1172 (m), 1120 (m), 1062 (m), 942 (s), 920 (sh), 793 (w), 753 (w), 621 (sh), 533 (s), 469 (s).

The red brown microcrystals represent a different compound, $[\{Co(N(CH_2)_4N)\}V_2O_6]$ (**2**). X-ray diffraction quality crystals of compound **2** could be synthesized in a monophasic form by the following method.

Synthesis of $[\{Co(N(CH_2)_4N)\}V_2O_6]$ (2). A mixture of V_2O_5 (1.25 mmol), $LiOH{\cdot}H_2O$ (2.5 mmol), pyrazine (1.87 mmol), $CoSO_4{\cdot}7H_2O$ (1.87 mmol), and H_2O (555.55 mmol) in the molar ratio of 1:2:1.5:1.5:444 was placed in a 23 mL Teflon-lined Parr autoclave. The mixture was stirred for 30 s and heated for 72 h at 135 °C inside an electric furnace. After the autoclave was cooled to room temperature for 3 h, reddish brown prismatic crystals mixed with a brown powder were filtered from the light pink color mother liquor. The mixture was washed thoroughly with methanol and then

(17) (a) Khan, M. I.; Cevik, S.; Doedens, R. In *Polyoxometalate Chemistry for Nano-Composite Design*; Yamase, T., Pope, M. T., Eds.; Kluwer Academic: New York, 2002; pp 27−38. (b) Khan, M. I.; Yohannes, E.; Ayesh, S.; Doedens, R. J. *J. Mol. Struct.* **2003**, *656*, 45−53. (c) Khan, M. I.; Yohannes, E.; Doedens, R. J. *Inorg. Chem.* **2003**, *42*, 3125−3129.
(18) (a) Khan, M. I.; Cevik, S.; Powell, D.; Li, S.; O'Connor, C. J. *Inorg. Chem.* **1998**, *37*, 81−86. (b) Khan, M. I.: Cevik, S.; Doedens. R. *J. Chem. Soc., Chem. Commun.* **2001**, 1930−1931 .
(19) (a) Khan, M. I.; Tabussum, S.; Doedens, R. J. *Chem. Commun.* **2003**, 532−533. (b) Khan, M. I.; Tabussum, S. and Doedens, R. J.; Golub, V. O.; O'Connor, C. J. *Inorg. Chem. Commun.* **2004**, *7*, 54.
(20) (a) Khan, M. I.; Yohannes, E.; Doedens, R. J. *Angew. Chem., Int. Ed.* **1999**, *38*, 1292. (b) Khan, M. I.; Hope, T.; Cevik, S.; Zheng, C.; Powell, D. *J. Cluster Sci.* **2000**, *11*, 433−447.
(21) (a) Khan, M. I.; Ayesh, S.; Yohannes, E.; Doedens, R. J. *Front. Biosci.* **2003**, *8*, 177−183. (b) Khan, M. I.; Giri, S.; Ayesh, S.; Doedens, R. J. *Inorg. Chem. Commun.* **2004**, *7/6*, 721−724.
(22) Khan, M. I.; Yohannes, E.; Nome, R.; Ayesh, S.; Golub, V. O.; O'Connor, C. J.; Doedens, R. J. *Chem. Mater.* **2004**, *16*, 5273−5279.
(23) (a) Khan, M. I.; Yohannes, E.; Doedens, R. J.; Golub, V. O.; O'Connor, C. J. *Inorg. Chem. Commun.* **2005**, *8*, 841−845. (b) Khan, M. I.; Deb S.; Golub, V. O.; O'Connor, C. J.; Doedens, R. J. *Inorg. Chem. Commun.* **2006**, *9*, 25−28.
(24) Khan, M. I.; Deb S.; Nome, R.; Yohannes, E.; Cevik, S.; Doedens, R. Unpublished work.
(25) (a) Pope, M. T. *Heteropoly and Isopoly Oxometalates*; Springer: Berlin, 1983. (b) Pope, M. T.; Müller, *A. Angew. Chem., Int. Ed.* **1991**, *30*, 34−48. (c) Pope, M. T. In *Comprehensive Coordination Chemistry II: From Biology to Nanotechnology*; Wedd, A. G., Ed.; Elsevier: Oxford, 2004; Vol. 4, pp 635−678. (d) Hill, C. L. In *Comprehensive Coordination Chemistry II: From Biology to Nanotechnology*; Wedd, A. G., Ed.; Elsevier: Oxford, 2004; Vol. 4, pp 679−759.
(26) (a) Bjornberg, A.; Hedman, B. *Acta Chem. Scand.* **1977**, *A31*, 579−584. (b) Hawthorne, F. C. *J. Solid State Chem.* **1997**, *22*, 157− 170. (c) Baudrin, E.; Touboul, M.; Nowogrocki, G. *J. Solid State Chem.* **2000**, *152*, 511−516.
(27) (a) Koene, B.; Taylor, N.; Nazar, L. *Angew. Chem., Int. Ed.* **1999**, *38*, 2888−2891 and references therein. (b) Shan, Y.; Huang, R.; Huang, S. *Angew. Chem., Int. Ed.* **1999**, *38*, 1751−1754.
(28) Dyer, A. *An Introduction to Zeolite Molecular Sieves*; Wiley: New York, 1988.
(29) Barrer, R. M. *Hydrothermal Chemistry of Zeolites*; Academic Press: London, 1982.
(30) O'Connor, C. J. *Prog. Inorg. Chem.* **1979**, *29*, 203.

with deionized water and dried at room temperature. The reddish brown prismatic crystals were separated from the brown powder mechanically to give ~398 mg of [{Co(N(CH)$_4$N)}V$_2$O$_6$] (**2**; 94.5% based on vanadium). Anal. Calcd for $C_4H_4N_2O_6CoV_2$ (**2**): C, 14.26; H, 1.19; N, 8.31; Co, 17.49; V, 30.24. Found: C, 14.01; H, 1.05; N, 8.13; Co, 14.03; V, 30.02. Prominent IR bands (KBr pellet, 4000−400 cm^{-1}): 1481(w), 1414 (s), 1163 (s), 1119 (s), 1087 (w), 1057 (s), 910 (vs), 817 (s), 789 (m), 756 (s), 631 (vs), 540 (vw), 475 (s).

Single-Crystal X-ray Diffraction Analyses. An X-ray quality crystal of each compound was selected. After the crystal was glued to a thin glass fiber with epoxy resin, it was mounted on a Bruker SMART-CCD[31] diffractometer equipped with graphite monochromatized Mo Kα radiation (λ = 0.710 73 Å). The X-ray data were collected at 163(2) K. The data were processed with the SAINT[32] software, and empirical absorption corrections were applied with SADABS.[33] All other calculations were performed by use of the SHELXTL[34] package. The structures were solved by direct methods and refined on F^2 by full-matrix least-square techniques.

Results and Discussion

Compounds **1**−**2** are readily isolated in moderate to high yields in highly crystalline forms from the hydrothermal reactions described in the experimental section. Reactions for the synthesis of **1** yielded large black crystals of compound **1** mixed with red brown microcrystals of **2** which could be separated readily. Slight modification in the reaction conditions, especially by lowering the reaction temperature and reaction time, resulted into the high yield synthesis of X-ray diffraction quality crystals of **1** in monophasic form. Theses crystals exhibit shiny faces. They are stable in air, insoluble in cold and hot water, and common organic solvents.

The infrared spectra of [{Co(N(CH)$_4$N)}(V$_2$O$_5$)$_2$] (**1**) and [{Co(N(CH)$_4$N)}V$_2$O$_6$] (**2**) exhibit a series of bands associated with the pyrazine ring which, unlike other aromatics,[35−38] usually lie below 1500 cm^{-1}. The bands between 1300 and 1000 cm^{-1} due to in-plane C−H bending and ring deformation slightly shifted to higher frequencies. This is characteristic of pyrazine coordinated to metal centers.[37]

The infrared spectra of the two compounds also contain several bands in the lower frequency region. The positions of these bands differ significantly for the two compounds, indicating different structures for **1** and **2**. For [{Co(N(CH)$_4$N)}(V$_2$O$_5$)$_2$] (**1**), the strong band at 942 cm^{-1} and a shoulder at 920 cm^{-1} are assigned to ν(V═O). Multiple bands at 793 (w), 753 (m), 621 (s), 533 (s), and 469 (vw) cm^{-1} correspond to asymmetric and symmetric stretching vibrations of the bridging metal oxide groups. The infrared spectrum of [{Co(N(CH)$_4$N)}V$_2$O$_6$] (**2**) shows bands that resemble the characteristic IR absorption bands of metavanadates.[39] The bands at 910 (vs) cm^{-1} and 817 (s) cm^{-1} are assigned to symmetric and asymmetric (V═O) stretching. Additional bands at 789 (m), 756 (s), 631 (vs), and 540 (w) cm^{-1} are attributable to (V−O−V) stretching of the metavanadate backbone of the compound. These assignments are consistent with other published literature.[39,40]

The results of the redox titration performed on each compound indicate that compound **2** does not contain any reduced vanadium (IV) sites whereas compound **1** has two reduced (V^{IV}) sites per formula unit. These results are consistent with the bond valence sum calculations[41] and charge balance requirements of the compounds.

Compound **1** crystallizes in the orthorhombic space group *Cmcm*. Crystallographic data, atomic coordinates, and selected bond distances and bond angles are given in Tables 1−3. Single-crystal X-ray diffraction analysis revealed a three-dimensional framework structure. A view of the

Table 1. Crystallographic Data for [{Co(N(CH)$_4$N)}(V$_2$O$_5$)$_2$] (1) and {Co(N(CH)$_4$N)}V$_2$O$_6$] (2)

	[{Co(N(CH)$_4$N)}(V$_2$O$_5$)$_2$] (**1**)	[{Co(N(CH)$_4$N)}V$_2$O$_6$] (**2**)
empirical formula	$C_4H_4CoN_2O_{10}V_4$	$C_4H_4CoN_2O_6V_2$
formula weight	502.78	336.90
crystal system	orthorhombic	orthorhombic
space group	*Cmcm*	*Pnna*
a (Å)	14.3071(6)	10.2524(8)
b (Å)	6.9965(3)	11.5653(9)
c (Å)	11.4510(5)	7.4719(6)
α [deg]	90	90
β [deg]	90	90
γ [deg]	90	90
V (Å^3)	1146.24(9)	885.96(12)
Z	4	4
T (K)	163(2)	163(2)
ρ_{calcd} (g·cm^{-3})	2.913	2.526
μ (mm^{-1})	4.614	3.925
final R$_1$,[a] wR2[b] [$I > 2\delta(I)$]	0.0381, 0.1017	0.0182, 0.0541
Final R$_1$,[a] wR2[b] (all data)	0.0385, 0.1019	0.0199, 0.0547

[a] $R1 = \sum||F_o| - |F_c||/\sum|F_o|$. [b] $wR2 = [\sum[w(F_o^2 - F_c^2)^2]/\sum[w(F_o^2)^2]]^{1/2}$.

Table 2. Atomic Coordinates (Å × 10^4) and Equivalent Isotropic Displacement Parameters (Å^2 × 10^3) for [{Co(N(CH)$_4$N)}(V$_2$O$_5$)$_2$] (1)

	x	*y*	*z*	*U*(eq)[a]
Co(1)	0	1748(2)	2500	6(1)
V(1)	2125(1)	1353(1)	3969(1)	7(1)
O(1)	1004(2)	1752(5)	3778(3)	10(1)
O(2)	2282(3)	1287(4)	5693(3)	13(1)
O(3)	2592(3)	1177(6)	2500	10(1)
N(1)	0	4757(11)	2500	9(2)
N(2)	0	8745(11)	2500	9(2)
C(1)	0	7739(12)	3464(7)	39(3)
C(2)	0	5752(12)	3459(7)	50(4)

[a] *U*(eq) is defined as one-third of the trace of the orthogonalized U_{ij} tensor.

(31) *SMART*, Version 4.210; Simens Analytical X-Ray Systems: Madison, WI, 1997
(32) *SAINT*, Version 4.050; Simens Analytical X-Ray Systems: Madison, WI, 1995.
(33) . Sheldrick, G. M. *SADABS*; University of Gottingen: Gottingen, Germany, 1997.
(34) . Sheldrick, G. M. *SHELXTL*, Version 5.1; Siemens Industrial Automation, Inc.: Madison, WI, 1995.
(35) Bellamy, L. J. *The Infrared Spectra of Complex Molecules*; John Wiley & Sons: New York, 1975; pp 279−320.
(36) Lord, R. C.; Warston, A. L.; Miller, F. A. *Spectrochim. Acta* **1957**, *9*, 113−125.
(37) Ferraro, J. R. *Low-Frequency Vibration of Inorganic and Coordination Compounds*; Plenum Press: New York, 1971; pp 191−246.
(38) Topacli, A. *Spectrochim. Acta* **1995**, *51A*, 633−641.
(39) Waal, D.; Heyns, A. M. *Mater. Res. Bull.* **1992**, *27*, 129−136.
(40) Wery, A. S. J.; Zorrilla, J. M. G.; Luque, A.; Ugalde, M.; Roman, P. *Chem. Mater.* **1996**, *8*, 408−413.
(41) Brown, I. D.; Wu, K. K. *Acta Crystallogr.* **1976**, *B32*, 1957−1959.

Table 3. Selected Bond Lengths [Å] and Bond Angles [deg] for [{Co(N(CH)4N)}(V2O5)2] (1)[a]

Co1−O1	2.051(3)	V1−O2 (#5)	1.897(3)
Co1−N1	2.105(8)	V1−O2 (#6)	1.900(3)
Co1−N2 (#4)	2.101(8)	V1−O3	1.814(2)
V1−O1	1.643(3)	V1−V1 (#5)	3.051(2)
V1−O2	1.988(3)	V1−V1 (#6)	3.027(2)
O1−Co1−O1 (#1)	179.9(2)	O2−V1−O2 (#5)	76.5(2)
O1−Co1−O1 (#2)	88.9(2)	O2−V1−O2 (#6)	76.2(2)
O1−Co1−N1	88.93(10)	O3−V1−O2 (#5)	94.8(2)
N1−Co1−N2 (#4)	180.0	O3−V1−O2 (#6)	94.6(2)
O1−V1−O2	104.2(2)		
O1−V1−O2 (#5)	108.4(2)	V1−O2−V1 (#5)	103.5(2)
O1−V1−O2 (#6)	107.9(2)	V1−O2−V1 (#6)	102.2(2)
O1−V1−O3	104.4(2)	V1 (#5)−O2−V1 (#6)	149.0(2)
O2 (#5)−V1−O2 (#6)	138.7(1)	V1−O3−V1 (#3)	136.0(3)
O2−V1−O3	151.4(2)		

[a] Symmetry transformations used to generate equivalent atoms: #1, $-x$, y, $-z+1/2$; #2, $-x$, y, z; #3, x, y, $-z+1/2$; #4, x, $y-1$, z; #5, $-x+1/2$, $-y+1/2$, $-z+1$; #6, x, $-y$, $-z+1$; #7, x, $y+1$, z.

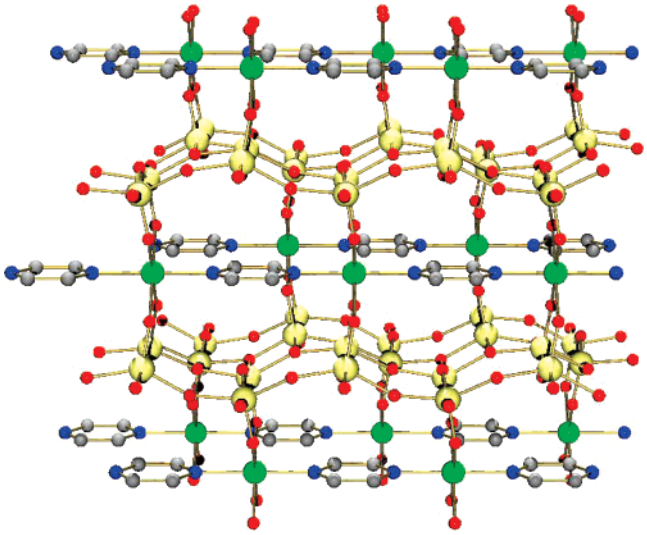

Figure 1. View of the extended structure of [{Co(N(CH)4N)}(V2O5)2] (**1**) showing alternating corrugated {V2O5} layers and polymeric coordination complex linkers. (Hydrogen atoms are omitted for clarity. Atom color codes: yellow, V; green, Co; blue, N; red, O; gray, C).

extended structure of the neutral composite framework is shown in Figure 1. It consists of alternating layers, perpendicular to the *c*-axis, of vanadium oxide and cobalt−pyrazine.

The vanadium oxide layers in **1** are constructed from {VO_5} square pyramids sharing edges and corners, similar to those found in pure V_2O_5.[42] However, unlike the neutral vanadium oxide layers in V_2O_5 which contain only fully oxidized vanadium(V) centers, the vanadium oxide layers in **1** contain mixed-valence vanadium (IV/V) centers, conferring a formal negative charge to these layers.[43] The interleaved cobalt−pyrazine layers, which are composed of $\{Co(N(CH)_4N)\}_n^{2n+}$ chains, have a formal positive charge. Besides cross-linking the successive vanadium oxide layers

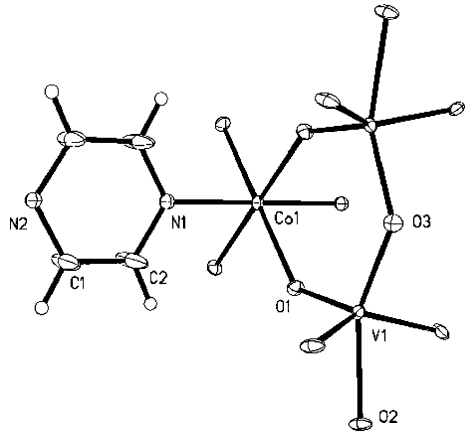

Figure 2. Building unit in the crystal structure of [{Co(N(CH)4N)}(V2O5)2] (**1**) showing the atom labeling scheme and 50% displacement ellipsoids.

by forming {−V−O−Co−O−V−} linkages, the cobalt−pyrazine cationic layers thus provide the charge balance to generate the neutral framework in **1**. The framework structure in **1** can alternatively be viewed as composed of reduced and negatively charged layers of {V_2O_5} intercalating $\{Co(N(CH)_4N)\}_n^{2n+}$ layers and held together by host−guest interactions.[44,45]

A building block unit of the structure showing the coordination environment and atom labeling scheme in [{Co(N(CH)4N)}(V2O5)2] is shown in Figure 2. The octahedral geometry about each cobalt center is defined by two nitrogen donor atoms from pyrazine ligands and four oxygen atoms derived from the two adjacent vanadium oxide layers. Co−N bond distances (2.101(8)−2.105(8) Å) and Co−O bond distances (2.051(3) Å) are in the expected range (Table 3). The square pyramidal geometry around vanadium in each {VO_5} unit is defined by three μ_3 oxygen atoms and one μ_2 oxygen atom (V−O = 1.814(2)−1.988(3) Å) that are employed in edge-sharing and corner sharing, respectively, with five other {VO_5} units in the same V/O layer and a terminal oxygen atom (V−O = 1.643(3) Å). The terminal oxygen, in turn, is bonded to a cobalt center of the adjacent cobalt−pyrazine layer, cross-linking the layers. The somewhat elongated displacement ellipsoids of the pyrazine carbons are indicative of a small degree of rotational disorder of the six-membered rings.

The crystallographic data, atomic coordinates, and selected bond distances and bond angles for compound **2** are given in Tables 1, 4, and 5, respectively. It crystallizes in the orthorhombic space group *Pnna*. Figure 3 shows a view of the extended neutral framework structure in the crystals of **2**. It differs significantly from the structure of **1**. The hybrid framework in **2** consists of vanadium oxide chains, which are cross-linked into a three-dimensional structure by coordination polymers $\{Co(N(CH)_4N)\}_n^{2n+}$. The vanadium oxide chains, composed of corner sharing {VO_4} tetrahedra, are reminiscent of metavanadates. The vanadium centers of the {VO_4} units in the chain are in a distorted tetrahedral environment, with V−O bond lengths in the 1.6523−1.7958

(42) Enjalbert, R.; Gally, J. *Acta Crystallogr.* **1986**, *C42*, 1467−1469.
(43) In space group *Cmcm*, the asymmetric unit contains a single vanadium atom, which lies on a 16-fold general position. Magnetic data, redox titrations, bond valence sum calculations, and charge balance considerations lead to the conclusion that this site contains equal proportions of V(IV) and V(V). Attempted refinement of the structure in the alternative noncentrosymmetric space groups *Ama*2 and *Cmc*2_1 showed typical problems associated with attempted refinement of a centrosymmetric structure in a noncentrosymmetric subgroup: large correlations, large parameter shifts, higher *R*-values, and non-positive definite displacement parameters.
(44) Shan, Y.; Huang, R.; Huang, S. D. *Angew. Chem., Int. Ed.* **1999**, *38*, 1751−1754.
(45) Kanatzidis, M. G.; Wu, C.-G. *J. Am. Chem. Soc.* **1989**, *111*, 4139−4141.

Table 4. Atomic Coordinates (Å × 10⁴) and Equivalent Isotropic Displacement Parameters (Å² × 10³) for [{Co(N(CH)₄N)}V₂O₆] (2)

	x	*y*	*z*	*U*(eq)[a]
Co(1)	10728(1)	2500	2500	7(1)
V(1)	7748(1)	1462(1)	984(1)	8(1)
O(1)	9334(1)	1709(1)	888(1)	11(1)
O(2)	7500	0	1718(2)	14(1)
O(3)	7058(2)	2500(1)	2500	12(1)
O(4)	7129(1)	1674(1)	−1036(1)	12(1)
N(1)	10444(1)	3993(1)	838(2)	11(1)
C(1)	10630(1)	5042(1)	1565(2)	13(1)
C(2)	9809(2)	3960(1)	−727(2)	13(1)

[a] *U*(eq) is defined as one-third of the trace of the orthogonalized U_{ij} tensor.

Table 5. Selected Bond Lengths [Å] and Bond Angles [deg] for [{Co(N(CH)₄N)}V₂O₆] (2)[a]

Co1−O1	2.0807(11)	V1−O2	1.7957(6)
Co1−O4 (#1)	2.0434(11)	V1−O3	1.7958(7)
Co1−N1	2.1472(13)	V1−O4	1.6548(11)
V1−O1	1.6523(11)		
O1−Co1−O1 (#3)	93.25(6)	O4 (#2)−Co1−N1	99.30(5)
O1−Co1−O4 (#1)	176.89(4)	N1−Co1−N1 (#3)	164.45(7)
O1−Co1−O4 (#2)	88.13(4)	V1−O1−Co1	136.62(6)
O4 (#1)−Co1−O4 (#2)	90.62(6)	V1−O2−V1 (#4)	144.42(10)
O1−Co1−N1	85.74(5)	V1−O3−V1 (#3)	133.63(10)
O4 (#1)−Co1−N1	91.65(5)	V1−O4−Co1 (#5)	145.80(10)

[a] Symmetry transformation used to generate equivalent atoms: #1, $x + 1/2, -y + 1/2, z + 1/2$; #2, $x + 1/2, y, -z$; #3, $x, -y + 1/2, -z + 1/2$; #4, $-x + 3/2, -y, z$; #5, $x - 1/2, y, -z$; #6, $-x + 2, -y + 1, -z$.

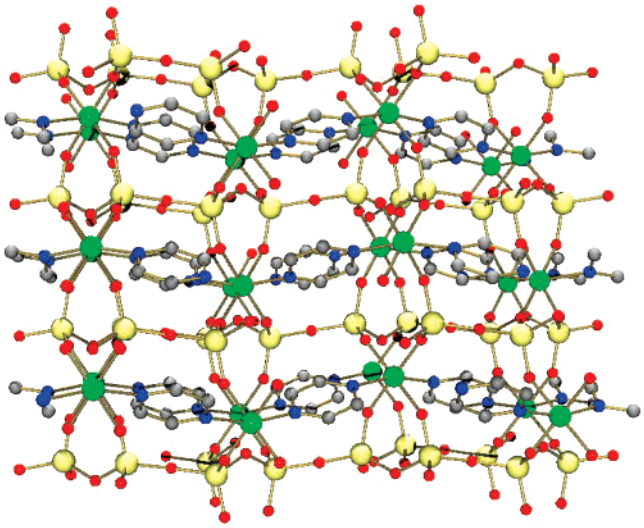

Figure 3. View of the extended structure of [{Co(N(CH)₄N)}V₂O₆] (**2**) showing vanadium oxide chains and polymeric coordination complex cross-linkers. (Hydrogen atoms are omitted for clarity. Atom color codes: yellow, V; green, Co; blue, N; red, O; gray, C).

Å range and {O−V−O} bond angles ranging from 108.19° to 112.39° (Table 5). Each {VO_4} unit shares two oxygen atoms with two adjacent {VO_4} units in the chain. The remaining two oxygen atoms are shared with two different cobalt atoms that are part of $\{Co(N(CH)_4N)\}_n^{2n+}$ chains lying above and below the vanadium oxide chain.

Each pyrazine ligand in the $\{Co(N(CH)_4N)\}_n^{2n+}$ chain is coordinated to two cobalt centers through its two nitrogen atoms to form a one-dimensional cationic complex chain, which runs parallel to the metavanadate chains. Each cobalt center in the polymeric chain is linked to two adjacent vanadium atoms in the same metavanadate chain and to two other vanadium atoms in two different chains through corner

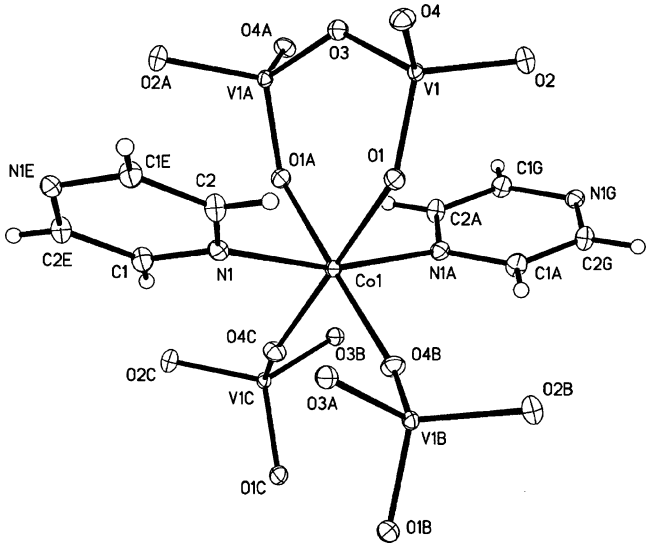

Figure 4. building block unit in the crystal structure of [{Co(N(CH)₄N)}-V₂O₆] (**2**) showing the atom labeling scheme and 50% displacement ellipsoids.

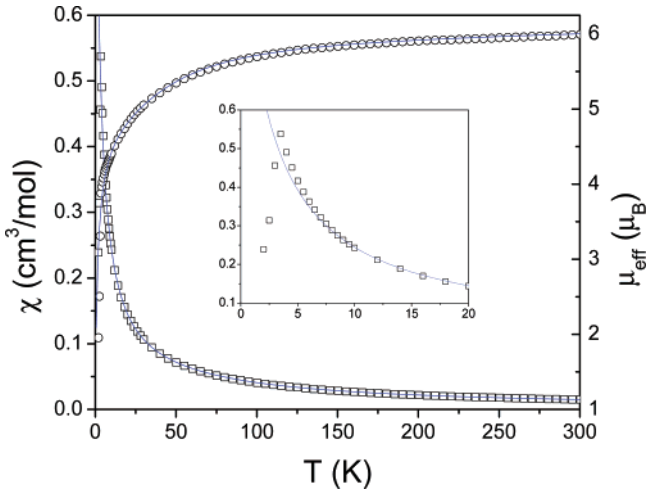

Figure 5. Dependences of the magnetic susceptibility χ (□) and effective magnetic moment μ_{eff} (○) of the [{Co(N(CH)₄N)}(V₂O₅)₂] compound on temperature *T*. The line drown through the data is the fit to eq 1 (see text).

shared oxygen atoms. Thus, each cationic $\{Co(N(CH)_4N)\}_n^{2n+}$ chain cross-links three different metavanadate chains, $\{V_2O_6\}_n^{2n-}$, to generate a neutral three-dimensional mixed metal oxide hybrid framework.

As shown in Figure 4, the distorted octahedral geometry around the cobalt center is defined by four oxygen atoms from three vanadium oxide chains (Co−O = 2.0434(11)−2.0807(11) Å) and two nitrogen donor atoms from two pyrazine ligands in the same Co−pyrazine chain (Co−N = 2.1472(13) Å). The cis and trans bond angles range from 85.74(5) to 99.30(5)° and from 164.45(7) to 176.89(4)°, respectively (Table 5). The C−C and C−N distances in the pyrazine ring are in the expected range.

The TGA of [{Co(N(CH)₄N)}(V₂O₅)₂] (**1**) revealed the remarkable thermal stability of the compound. The TGA plot shows that the hybrid framework of the material is stable up to 282 °C. Above this temperature, it starts decomposing with multiple step weight losses, which continue up to 565 °C leaving a black residue. The weight loss in the temperature range 431−560 °C corresponds to the loss of

all organics (one pyrazine per formula unit). The TGA of [{Co(N(CH)$_4$N)}V_2O_6] (**2**) showed a similar multistep weight loss pattern in the temperature range 225−553 °C. Here, a two-step weight loss in the temperature range 420−553 °C corresponds to the loss of one pyrazine molecule per formula unit. The IR spectra showed that the black residues left after the TGA experiments in both cases are likely to be mixed metal oxide {Co/V/O} phases which were not characterized further.

Magnetic data for [{Co(N(CH)$_4$N)}$(V_2O_5)_2$] (**1**) are represented in Figure 5. The effective moment of the compound increases with increasing temperature, which is characteristic for cobalt(II) containing compounds. Around 3.5 K a sharp peak in the susceptibility dependence is observed which is probably connected with antiferromagnetic ordering. The effective magnetic moment at 300 K is 5.99 μ_B. The description (for temperatures above 10 K) of the experimental results used the equation for zero field splitting of spin multiplets ($S = 3/2$) for Co^{2+}, taking into account the presence of two V^{+4} ions per formula unit:

$$\chi = \chi_0 + \chi_{TI} = \frac{N_A g_{Co}{}^2 \mu_B{}^2}{k_B T} \frac{3 + 2/x + (3 - 2/x)e^{-2x}}{4(1 + e^{-2x})} + 2\frac{N_A g_V{}^2 \mu_B{}^2}{4k_B T} + \chi_{TI} \quad (1)$$

where $x = D/k_BT$. The calculated susceptibility χ has been corrected for exchange interaction zJ' between spins:

$$\chi' = \frac{\chi_0}{1 - (2zJ'/N_A g^2 \mu_B{}^2)\chi} \quad (2)$$

Taking the typical value of $g_V = 1.97$, the best fit was $g_{Co} = 2.80$, $D/k_B = 76$ K, $zJ'/k_B = -0.45$ K, and $\chi_{TI} = 0.00063$ cm^3/mol.

Conclusions

The amalgamation of vanadium oxide chains and layers with metal−organoamine complexes resulted in the synthesis of inorganic−organic neutral framework materials: [{Co(N(CH)$_4$N)}$(V_2O_5)_2$] (**1**) and [{Co(N(CH)$_4$N)}V_2O_6] (**2**). Besides cross-linking the metal oxide chains and layers in these materials, cationic metal−organoamine polymers provide charge balance leading to the neutral frameworks. This synthetic approach is potentially applicable for combining a range of transition metal oxides with organoamines to produce a variety of hybrid materials. Compound **1** exhibits magnetic property that is characteristic for cobalt(II) containing compounds. The compounds reported here are among the very few known mixed metal oxide hybrids. They could be viewed as models for further studies leading to design and synthesis of new materials.

Acknowledgment. This work was partially supported by grants (to M.I.K.) from the American Chemical Society's Petroleum Research Fund (ACS-PRF#35591-AC5) and from the NSF (CHE-0210354). The magnetic measurement work at the University of New Orleans was partially supported by Grant NSF/LEQSF (2001-04)-RII-03.

Supporting Information Available: X-ray crystallographic files in CIF format for the structure determinations of [{Co(N(CH)$_4$N)}$(V_2O_5)_2$] (**1**), [{Co(N(CH)$_4$N)}V_2O_6] (**2**). This material is available free of charge via the Internet at http://pubs.acs.org. Details of the crystallographic data have also been deposited (CCDC reference number: [{Co(N(CH)$_4$N)}$(V_2O_5)_2$] (**1**), CCDC 644518; [{Co(N(CH)$_4$N)}V_2O_6] (**2**), CCDC 644519) with the Cambridge Crystallographic Data Center, 12 Union Road, Cambridge CB21EZ, U.K. (deposit@CCDC.cam.ac.uk).

CM071415N